# Position and spin control by dynamical ultrastrong spin-orbit coupling

C. Echeverría-Arrondo[1] and E. Ya. Sherman[1,2]
[1]*Department of Physical Chemistry, Universidad del País Vasco UPV/EHU, 48080 Bilbao, Spain*
[2]*IKERBASQUE, Basque Foundation for Science, Bilbao, Spain*
(Received 21 December 2012; published 30 October 2013)

Focusing on the efficient probe and manipulation of single-particle spin states, we investigate the coupled spin and orbital dynamics of a spin-1/2 particle in a harmonic potential subject to ultrastrong spin-orbit interaction and external magnetic field. The advantage of these systems is the clear visualization of the strong spin-orbit coupling in the orbital dynamics. We also investigate the effect of a time-dependent coupling: Its nonadiabatic change causes an interesting interplay of spin and orbital motion which is related to the direction and magnitude of the applied magnetic field. This result suggests that orbital state manipulation can be realized through ultrastrong spin-orbit interactions, becoming a useful tool for handling entangled spin and orbital degrees of freedom to produce, for example, spin-desirable polarizations in time that are interesting for spintronics implementations.

DOI: 10.1103/PhysRevB.88.155328 PACS number(s): 72.25.Rb, 03.67.Bg, 71.70.Ej, 73.63.Kv

## I. INTRODUCTION

Spin-orbit interactions have been proven very useful for realization of spintronics[1] with electrons in nanosystems. On the one hand, it has been demonstrated in theory and experiment that spins can be tuned by various electric means.[2–7] On the other hand, since spin-orbit coupling entangles spin and orbital motion, spin readout is reachable by electric means.[8] Such a combination points to the possibility of probing and manipulating spins hosted by semiconductor quantum dots[9,10] using only electric fields.[5] The spin-orbit control of qubits is a promising tool that suggests the investigation of the ultrastrong spin-orbit coupling regime to see all the features of this technique. Extreme spin-orbit interactions can be achieved at the surfaces of semiconductors coated with heavy metals (see, e.g., Refs. 11 and 12), which allow for spin manipulation by electric fields.[13,14] Recently, Rashba performed a detailed analysis of two-dimensional quantum dots with the ultrastrong spin-orbit coupling.[15] Very recently, it was recognized that fully controllable strong interactions, greatly beyond the range reachable in semiconductors, can be produced in ultracold atomic Bose and Fermi gases by optical means.[16,17] Similar to electrons in quantum dots, cold atoms are located in harmonic traps and can demonstrate controllably modified time-dependent spin-orbit coupling, opening new venues for studies of related dynamics.

The spin dynamics in these systems can be studied theoretically by analyzing the interaction between a harmonic oscillator and a two-level spin, making it similar to the Jaynes-Cummings model in quantum optics, as suggested by Debald and Emary.[18] This is a wide-purpose model (see, e.g., Refs. 19–21) applied in different fields of condensed-matter physics and quantum optics, such as cavity quantum electrodynamics, trapped ions, and superconducting qubits (see Refs. 22 and 23 for recent results). In addition, carbon nanotubes holding electron spins deeply coupled to the vibrational modes[24] can be described with the Jaynes-Cummings model.

The systems with spin-orbit couplings have several advantages not applicable elsewhere. We mention just two. First, the coordinate dependence of the spin density makes it possible to visualize the effects of strong coupling in terms of particle position and measurable spin densities. Second, spin-orbit interaction and the Zeeman field can be made time dependent,[25–27] making the relevant dynamics in both spin and coordinate spaces accessible. These effects provide strongly nontrivial extensions of the conventional Jaynes-Cummings model.

In a quantum dot, a spin-orbit strength $\alpha = \xi e\mathcal{E}_z$, where $\xi$ is the material- and structure-dependent constant, can be induced by applying an external electric field $\mathcal{E}_z$;[28] a scheme for the experimental setup is given in Fig. 1. In cold atomic gases this time-dependent modification can be reached by changing the amplitudes and geometries of the corresponding laser fields.

In this paper, we present a description of the spin dynamics of an electron in a semiconductor quantum dot or trapped cold atoms, subject to strong spin-obit interactions. We focus on a one-dimensional harmonic oscillator with a spin degree of freedom, capturing the main physics of the systems of interest. This oscillator is under an applied magnetic field which one can rotate with respect to the coordinate axes. We consider two types of spin-orbit couplings, constant and time dependent; the results given below thereby acquire wider application.

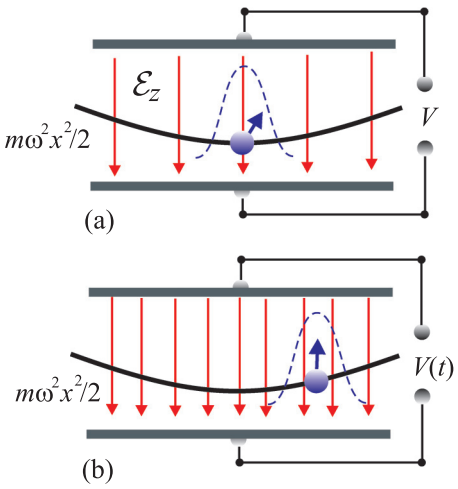


FIG. 1. (Color online) (a) Setup scheme for external generation of spin-orbit coupling through a bias voltage. Thick solid curves indicate the confining parabolic potential. (b) A nonadiabatic time-dependent field can cause electron displacement with spin rotation.

 

## II. HAMILTONIAN, EIGENSTATES, AND OBSERVABLES

The eigenstates can be obtained from the following Hamiltonian:

$$\hat{H}(t) = \hbar^2 k^2/2m + m\omega^2 x^2/2 + \alpha(t)\sigma_x k + \frac{\Delta}{2}\sigma_\Delta, \quad (1)$$

where $m$ is the particle effective mass, $\Delta$ and $\theta$ are the Zeeman splitting and tilt angle of the magnetic field as applied in the $xz$ plane, respectively, $\sigma_\Delta = \sigma_x \sin\theta + \sigma_z \cos\theta$ is the corresponding spin projection, and $\sigma_x$,$\sigma_z$ are the Pauli matrices. In the second quantization this Hamiltonian reads

$$\hat{H} = \hbar\omega(\hat{a}^\dagger\hat{a} + 1/2) + i\hbar\omega g(t)(\hat{a}^\dagger - \hat{a})\sigma_x + \frac{\Delta}{2}\sigma_\Delta, \quad (2)$$

where $\hat{a}^\dagger$ and $\hat{a}$ are the creation and annihilation operators, respectively, and $g = \alpha\sqrt{m/2\hbar^3\omega}$ is a dimensionless coupling constant, which can be understood as the ratio of the characteristic anomalous spin-dependent velocity $\alpha/\hbar$ to the characteristic quantum velocity spread in the ground state of the harmonic oscillator $\sqrt{\hbar\omega/m}$ or as the ratio of the quantum oscillator length $l_0 = \sqrt{\hbar/m\omega}$ to the spin precession length $\hbar^2/m\alpha$. We use the basis of spin orbitals $|n\rangle|\sigma\rangle$, composed of the eigenstates of $\hat{a}^\dagger\hat{a}$, $|n\rangle$, and those of $\sigma_z$, $|\sigma\rangle \equiv |\uparrow\rangle_z$, and $|\downarrow\rangle_z$ with respect to the $z$ axis. Numerical values of $g$ strongly vary from system to system. For InSb-based quantum dots, where $\alpha$ can reach $10^{-5}$ meV cm, $m$ is of the order of 0.02 of the free electron mass, and $\omega \sim 10^{12}$ s$^{-1}$, one can expect $g \approx 1$. For cold fermions such as $^{40}$K, where $\alpha/\hbar$ can be of the order of 10 cm/s and $\omega \sim 10^3$ s$^{-1}$, $g$ can be of the order of 10.

To make a connection to previous works on the ultrastrong regime (see, e.g., Ref. 19), first we investigate the effect of a constant coupling. The eigenstates of the full Hamiltonian $|\phi_i\rangle$ have the form $\sum_n |n\rangle(c_n^{\rm u}|\uparrow\rangle_z + c_n^{\rm d}|\downarrow\rangle_z)$, with the expansion coefficients $c_n^{\rm u}$ and $c_n^{\rm d}$; the normalized orbitals are expressed in the $x$ representation as

$$\langle x|n\rangle = \sqrt[4]{\frac{1}{\pi l_0^2 2^{2n}(n!)^2}}\exp\left[-\frac{x^2}{2l_0^2}\right]H_n\left[\frac{x}{l_0}\right], \quad (3)$$

where $H_n$ is the $n$th-order Hermite polynomial. In the limit of a very weak coupling, $g \ll 1$, in an arbitrarily directed magnetic field, $|\phi_i\rangle$ contains five main contributions. The main one is the direct product of $|n\rangle$ and the eigenstate of $\sigma_\Delta$. The other four are perturbative terms of direct products of $|n \pm 1\rangle$ and eigenstates of $\sigma_\Delta$. At $\theta = 0$, corresponding to the conventional Jaynes-Cummings model, spin selection rules exclude two of these four states. Moreover, at $\theta = 0$, in the eigenstates the contributions with different spatial parities have opposite spins. The expectation value of the velocity in the eigenstates is zero, $\langle v\rangle = d\langle x\rangle/dt = 0$; however, the mean momentum is finite:

$$\begin{aligned}\langle v\rangle &= \frac{i}{\hbar}\langle[H,x]\rangle = \frac{\hbar}{m}\langle k\rangle + \frac{\alpha}{\hbar}\langle\sigma_x\rangle = 0,\\ \langle k\rangle &= -\sqrt{2}\frac{g}{l_0}\langle\sigma_x\rangle.\end{aligned} \quad (4)$$

Correspondingly, for the coordinate, $\langle\phi_i|x|\phi_i\rangle = 0$. Equation (4) corresponds to zero mechanical momentum $\hbar k - \mathcal{A}$ for the gauge[29] $\mathcal{A} = -m\alpha\sigma_x/\hbar$. The total spectrum results from the magnetic field mixing of two parabolic branches; that for $\langle k\rangle = -\sqrt{2}g/l_0$ when the spin state is $|\uparrow\rangle_x$, and that for $\langle k\rangle = \sqrt{2}g/l_0$ when it is $|\downarrow\rangle_x$.

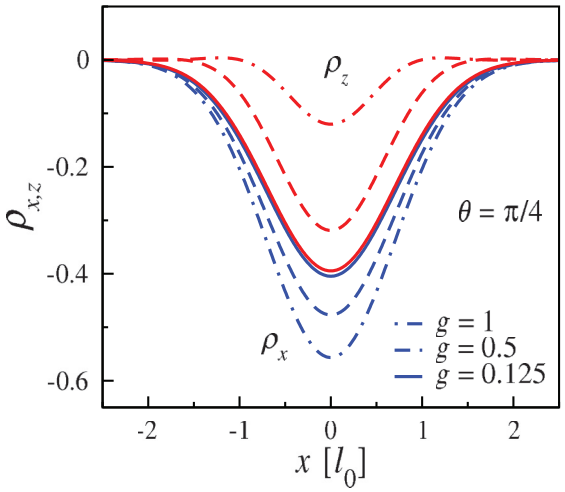


FIG. 2. (Color online) Nonzero spin densities $\rho_{x,z}$ for different $g$ values when the electron is at the ground state. Note that $\rho_x$ and $\rho_z$ merge for smaller $g$ coupling. Here and below we use a truncated Hilbert space of 64 states, which is sufficient to study ultrastrong spin-orbit coupling. The Zeeman splitting in all calculations is taken as $\Delta = 0.5\hbar\omega$.

To show the advantages of systems with spin-orbit coupling, we calculate the spatially resolved spin densities $\rho_j(x)$, $j = x,y,z$, providing valuable information about the system.[30] For an arbitrary state $|\psi\rangle$, presented in the form $\sum_n |n\rangle(a_n^{\rm u}|\uparrow\rangle_z + a_n^{\rm d}|\downarrow\rangle_z)$, these functions are defined as

$$\rho_j(x) = \sum_{n,m}\langle n|x\rangle\langle x|m\rangle\left(a_n^{\rm u*}, a_n^{\rm d*}\right)\sigma_j\begin{pmatrix}a_m^{\rm u}\\ a_m^{\rm d}\end{pmatrix}. \quad (5)$$

We focus on a particle in the ground state and take $\theta = \pi/4$ as an example. The densities $\rho_j(x)$ are presented in Fig. 2. The integrals of $\rho_j(x)$ over the $x$ coordinate are the spin expectation values.

## III. COUPLED SPIN AND COORDINATE DYNAMICS

Next, we analyze the coupled dynamics of a system in a state initially different from an eigenstate of the Hamiltonian in Eq. (2). For this purpose, we choose as a typical example an eigenstate of $\sigma_\Delta$ antiparallel to the magnetic field:

$$|\psi(0)\rangle = |0\rangle[-\sin(\theta/2)|\uparrow\rangle_z + \cos(\theta/2)|\downarrow\rangle_z]. \quad (6)$$

The time dependence is obtained from $|\psi(t)\rangle = \sum_i \zeta_i|\phi_i\rangle e^{-iE_i t/\hbar}$, where $\zeta_i$ are the corresponding expansion coefficients. We study the dynamics of spin densities for $\theta = \pi/4$ and $g = 1$. The particle oscillations are shown in Fig. 3(a). The Gaussian-like shape of $\rho_x(x)$ is robust against time; however, those of $\rho_y(x)$ and $\rho_z(x)$ (not shown) are fully changed. As a consequence, we see a strong correlation between the spin state and the position of the particle even in the dynamical regime.

One of the main advantages of quantum dots and cold atoms is the ability to manipulate the strength of spin-orbit coupling and thus to cause dynamics in the orbital and spin channels. The time-dependent spin-orbit coupling can be used for the

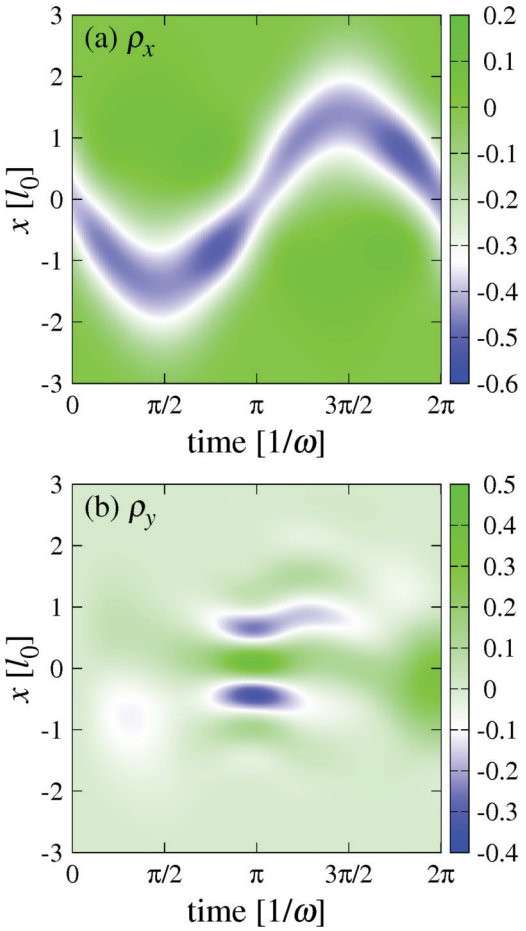


FIG. 3. (Color online) Spin densities (a) $\rho_x$ and (b) $\rho_y$ as a function of time for an electron spin antiparallel to the applied magnetic field with $\theta = \pi/4$; here we take the marginal case $g = 1$.

generation of spin currents in a two-dimensional electron gas[31] and spin separation in two-electron quantum dots similar to that predicted in Ref. 32. Here we take a single-period perturbation $g(t) = g_0 \sin(\Omega t)$ at frequency $\Omega$, which is fast enough to yield an appreciable nonadiabatic behavior but sufficiently slow to allow using the available electrical and optical means to generate the spin-orbit interaction. To clearly see the effects of strong spin-orbit coupling, we compare below the obtained numerically exact result with the perturbation theory.

To use the perturbation theory we take the basis of the first four eigenstates,

$$\begin{aligned} \psi_1 &= |0\rangle|\downarrow\rangle_z, \quad \psi_2 = |0\rangle|\uparrow\rangle_z, \\ \psi_3 &= |1\rangle|\downarrow\rangle_z, \quad \psi_4 = |1\rangle|\uparrow\rangle_z, \end{aligned} \tag{7}$$

where the time-dependent wave function becomes

$$\boldsymbol{\psi}(t) = a_1(t)\psi_1 + a_3(t)\psi_3 e^{-i\omega t} + a_4(t)\psi_4 e^{-i(\omega+\Delta)t}. \tag{8}$$

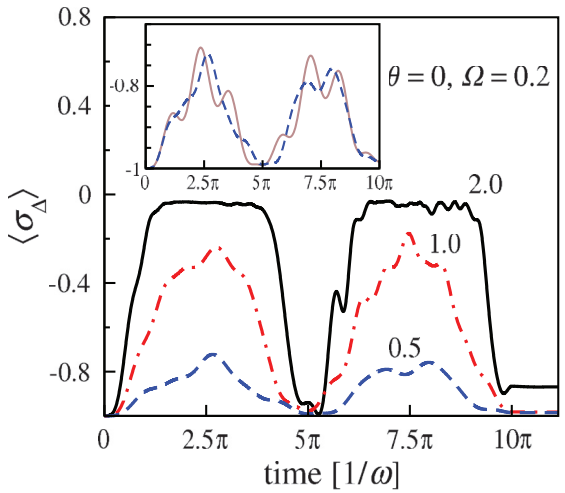


FIG. 4. (Color online) Dynamics of spins under a time-dependent $g(t) = g_0 \sin(\Omega t)$. Lines are marked by corresponding $g_0$ values. The inset shows a comparison of the exact (dashed line) and perturbation-theory (solid line) results for $g_0 = 0.5$.

The assumed time dependence yields the expansion coefficients

$$a_3(t) = -g_0 \sin\theta \int_0^t \sin(\Omega\tau e^{i\omega\tau} d\tau, \tag{9}$$

$$a_4(t) = g_0 \cos\theta \int_0^t \sin(\Omega\tau) e^{i(\omega+\Delta)\tau} d\tau. \tag{10}$$

The expectation values of coordinate and spin projection onto the magnetic are expressed as

$$\langle x(t)\rangle \equiv \langle \boldsymbol{\psi}(t)|\,\widehat{x}\,|\boldsymbol{\psi}(t)\rangle = \frac{1}{\sqrt{2}}[a_3(t)e^{-i\omega t} + \text{c.c.}], \tag{11}$$

$$\langle \sigma_\Delta(t)\rangle \equiv \langle \boldsymbol{\psi}(t)|\,\sigma_\Delta\,|\boldsymbol{\psi}(t)\rangle = -1 + 2\left|a_4^2(t)\right|. \tag{12}$$

These perturbation-theory formulas show the role of the direction of magnetic field on the spin and spatial dynamics, which is not present in the conventional Jaynes-Cummings model and allows us to extend the abilities for coordinate and spin manipulation.

We treat the problem numerically for a single period $T = 2\pi/\Omega$,[33] beginning with $\theta = 0$, where Zeeman and spin-orbit fields are orthogonal, similar to the Jaynes-Cummings model. Figure 4 demonstrates the time dependence of $\langle\sigma_\Delta(t)\rangle$ for different couplings $g_0$ and shows a comparison with the perturbation result for $g_0 = 0.5$ in the inset. As can be seen in Fig. 4, spin projection at the magnetic field changes strongly with time, corresponding to the spin rotation due to the spin-orbit coupling, and remains constant, as expected, after the change stops. The value of this projection after the end of the perturbation corresponds to the degree of nonadiabaticity of this process. It is interesting to mention the appearance of plateaus at the strong spin-orbit-coupling regime. These plateaus show that even a low-frequency dynamics is strongly nonadiabatic. The reason is the following. In the presence of spin-orbit coupling and magnetic field with $\theta = 0$, the splitting of the ground-state doublet, $\Delta\exp(-2g^2) \ll \Delta$, is small due to weakly overlapping eigenstates in the momentum space, as

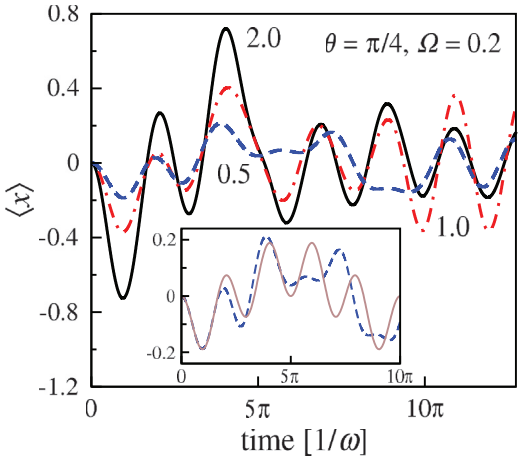


FIG. 5. (Color online) Dynamics of particle mean coordinate under time-dependent strength $g(t) = g_0 \sin(\Omega t)$. Lines are marked by corresponding $g_0$ values. The inset shows a comparison of the exact (dashed line) and perturbation-theory (solid line) results for $g_0 = 0.5$.

discussed after Eq. (4). As a result, even very slow changes in the system parameters cannot be treated adiabatically. Here spatial motion does not occur [$\langle x(t)\rangle = 0$], in agreement with Eq. (11).

Next, we take the state of Eq. (6), with $\theta = \pi/4$ as the initial one to demonstrate the qualitative role of the magnetic field direction. First, the qualitative effect is nonmonochromatic oscillations of the position, as depicted in Fig. 5. The oscillations in $\langle x(t)\rangle$ are caused mainly by transitions between the ground and first excited eigenstates of the model Hamiltonian; these states get mixed by the strong coupling. The amplitude of oscillations increases with $g_0$, as expected, and also with $\Omega$. The behavior strongly depends on the frequency and amplitude of spin-orbit coupling, as can be seen by comparing adiabatic and nonadiabatic plots. After the end of perturbation, the coordinate oscillates at frequency $\omega$. The next qualitative difference is in the behavior of $\langle\sigma_\Delta(t)\rangle$. Here, in the case of a strong static spin-orbit coupling, the splitting of the lowest doublet is $\Delta\cos\theta$. We see the effects of nonadiabatic perturbation and strong coupling in Fig. 6. Depending on $g_0$ and $\Omega$, different regimes in the dynamics of $\langle\sigma_\Delta(t)\rangle$ are possible: the system either returns to the initial state after the end of perturbation or switches to other states. The switching effect depends on the frequency of the field. At a small frequency, the dynamics is more adiabatic and perturbative, while for a larger frequency switching can occur. The insets in Figs. 5 and 6(a) show that the perturbation theory works if time is less than the oscillator period, while at longer times more states participate and the results become different. From this plot we can formulate the condition of strong spin-orbit coupling for a given system as a transition from peaklike ("weak" or "moderate" coupling) to steplike ("strong" coupling) evolution of $\langle\sigma_\Delta(t)\rangle$. It is interesting to mention that the transition and therefore the definition of the coupling strength in a dynamical system depend on the frequency of the applied external field.

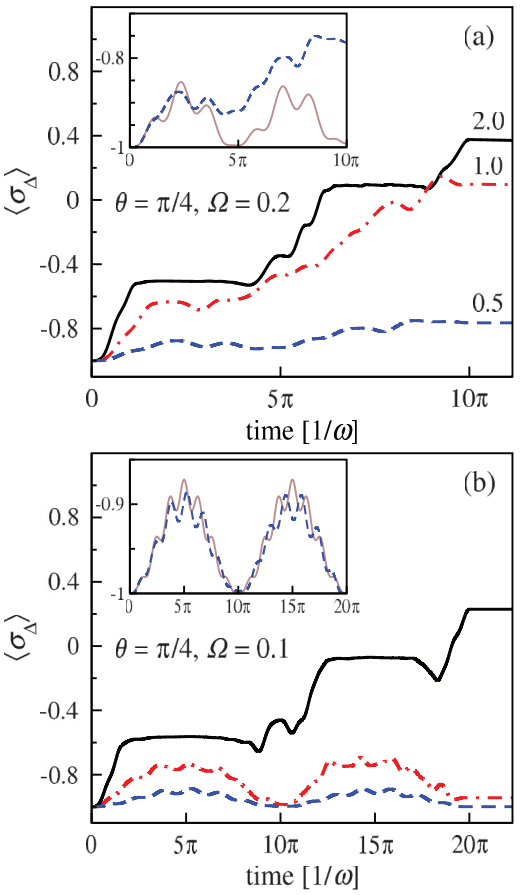


FIG. 6. (Color online) Dynamics of $\langle\sigma_\Delta\rangle$ under time-dependent strength $g(t) = g_0 \sin(\Omega t)$. Lines are marked by corresponding $g_0$ values. The initial state is the same as in Fig. 5. Insets show comparisons of the exact (dashed line) and perturbation-theory (solid line) results for $g_0 = 0.5$. (a) $\Omega = 0.2$ and (b) $\Omega = 0.1$.

## IV. CONCLUSIONS

In summary, we have investigated how strong dynamical spin-orbit couplings can be applied to probe and manipulate spins of electrons in semiconductor quantum dots and cold atoms in parabolic confinement through the correlated spin and orbital motion. We reveal the importance of the tilt angle of the applied magnetic field, an effect greatly beyond the conventional Jaynes-Cummings model. The obtained dynamics shows that, under a strong constant coupling, a particle oscillates in correlation with its spin orientation. The motion of the particle can be influenced by time-dependent coupling, with the result strongly dependent on all parameters. We observe a transition from periodic to steplike behavior of the spin component parallel to the magnetic field with increasing coupling strength. This fact clarifies the way to define the qualitative effect of ultrastrong spin-orbit coupling. The present work widens the applicability of spin-orbit control, as it covers different strengths for the induced interaction and tilt angles for the applied magnetic field. It also emphasizes the usability of electric and optical fields for spin probe and manipulation, which are crucial for spintronics. These results may also be of interest for quantum optics and quantum information realizations.

## ACKNOWLEDGMENTS

We gratefully acknowledge fruitful discussions with E. Il'ichev, G. Romero, E. Solano, and, especially, J. C. Retamal. We acknowledge support of the MINECO of Spain (Grant No. FIS 2009-12773-C02-01), the government of the Basque Country (grant "Grupos Consolidados UPV/EHU del Gobierno Vasco" IT-472-10), and the UPV/EHU (program UFI 11/55).



[1] I. Žutić, J. Fabian, and S. Das Sarma, Rev. Mod. Phys. **76**, 323 (2004); J. Fabian, A. Matos-Abiague, C. Ertler, P. Stano, and I. Zutic, Acta Phys. Slovaca **57**, 565 (2007).

[2] E. I. Rashba, Phys. Rev. B **78**, 195302 (2008); E. I. Rashba and Al. L. Efros, Phys. Rev. Lett. **91**, 126405 (2003).

[3] M. Governale, F. Taddei, and R. Fazio, Phys. Rev. B **68**, 155324 (2003).

[4] K. C. Nowack, F. H. L. Koppens, Yu. V. Nazarov, and L. M. K. Vandersypen, Science **318**, 1430 (2007).

[5] S. Nadj-Perge, S. M. Frolov, E. P. A. M. Bakkers, and L. P. Kouwenhoven, Nature (London) **468**, 1084 (2010).

[6] X. Hu, Y.-X. Liu, and F. Nori, Phys. Rev. B **86**, 035314 (2012).

[7] M. P. Nowak, B. Szafran, and F. M. Peeters, Phys. Rev. B **86**, 125428 (2012).

[8] L. S. Levitov and E. I. Rashba, Phys. Rev. B **67**, 115324 (2003).

[9] C. Echeverría-Arrondo, J. Pérez-Conde, and A. Ayuela, Appl. Phys. Lett. **95**, 043111 (2009).

[10] L. Besombes, Y. Léger, L. Maingault, D. Ferrand, H. Mariette, and J. Cibert, Phys. Rev. Lett. **93**, 207403 (2004).

[11] I. Gierz, T. Suzuki, E. Frantzeskakis, S. Pons, S. Ostanin, A. Ernst, J. Henk, M. Grioni, K. Kern, and C. R. Ast, Phys. Rev. Lett. **103**, 046803 (2009).

[12] K. Yaji, Y. Ohtsubo, S. Hatta, H. Okuyama, K. Miyamoto, T. Okuda, A. Kimura, H. Namatame, M. Taniguchi, and T. Aruga, Nat. Commun. **1**, 17 (2010).

[13] J. Ibañez-Azpiroz, A. Eiguren, E. Ya. Sherman, and A. Bergara, Phys. Rev. Lett. **109**, 156401 (2012).

[14] D. V. Khomitsky, J. Exp. Theor. Phys. **114**, 738 (2012).

[15] E. I. Rashba, Phys. Rev. B **86**, 125319 (2012).

[16] P. Wang, Z.-Q. Yu, Z. Fu, J. Miao, L. Huang, S. Chai, H. Zhai, and J. Zhang, Phys. Rev. Lett. **109**, 095301 (2012).

[17] L. W. Cheuk, A. T. Sommer, Z. Hadzibabic, T. Yefsah, W. S. Bakr, and M. W. Zwierlein, Phys. Rev. Lett. **109**, 095302 (2012).

[18] S. Debald and C. Emary, Phys. Rev. Lett. **94**, 226803 (2005).

[19] J. Casanova, G. Romero, I. Lizuain, J. J. García-Ripoll, and E. Solano, Phys. Rev. Lett. **105**, 263603 (2010), and references therein.

[20] J. Clarke and F. K. Wilhelm, Nature (London) **453**, 1031 (2008).

[21] D. Braak, Phys. Rev. Lett. **107**, 100401 (2011).

[22] S. Schmidt and G. Blatter, Phys. Rev. Lett. **104**, 216402 (2010), and references therein.

[23] Y. Hu and L. Tian, Phys. Rev. Lett. **106**, 257002 (2011), and references therein.

[24] A. Pályi, P. R. Struck, M. Rudner, K. Flensberg, and G. Burkard, Phys. Rev. Lett. **108**, 206811 (2012).

[25] O. Z. Karimov, G. H. John, R. T. Harley, W. H. Lau, M. E. Flatté, M. Henini, and R. Airey, Phys. Rev. Lett. **91**, 246601 (2003).

[26] P. S. Eldridge, W. J. H. Leyland, P. G. Lagoudakis, R. T. Harley, R. T. Phillips, R. Winkler, M. Henini, and D. Taylor, Phys. Rev. B **82**, 045317 (2010).

[27] A. Balocchi, Q. H. Duong, P. Renucci, B. L. Liu, C. Fontaine, T. Amand, D. Lagarde, and X. Marie, Phys. Rev. Lett. **107**, 136604 (2011).

[28] R. Winkler, *Spin-Orbit Coupling Effects in Two-Dimensional Electron and Hole Systems*, Springer Tracts in Modern Physics (Springer, Berlin, 2003).

[29] I. L. Aleiner and V. I. Fal'ko, Phys. Rev. Lett. **87**, 256801 (2001).

[30] D. V. Khomitsky and E. Ya. Sherman, Europhys. Lett. **90**, 27010 (2010).

[31] A. G. Malshukov, C. S. Tang, C. S. Chu, and K. A. Chao, Phys. Rev. B **68**, 233307 (2003).

[32] J. Pawlowski, P. Szumniak, A. Skubis, and S. Bednarek, arXiv:1309.5941.

[33] The dynamics are computed using a fourth-order Runge-Kutta method until $t = 2\pi/\Omega$ and using the decomposition $|\psi(t)\rangle = \sum_i \zeta_i |\phi_i\rangle e^{-iE_i t/\hbar}$ beyond that time.